Journal of Alloys and Compounds 505 (2010) 579–583

Contents lists available at ScienceDirect

Journal of Alloys and Compounds

journal homepage: www.elsevier.com/locate/jallcom

Preparation of TiO_2 films by layer-by-layer assembly and their application in solar cell

L. Zhang[a,b], A.J. Xie[a], Y.H. Shen[a,*], S.K. Li[a]

[a] School of Chemistry and Chemical Engineering, Anhui University, Hefei 230039, PR China
[b] Anhui Key Laboratory of Spin Electron and Nanomaterials (Cultivating Base), Suzhou University, Suzhou 234000, PR China

ARTICLE INFO

Article history:
Received 22 March 2010
Received in revised form 9 June 2010
Accepted 11 June 2010
Available online 23 June 2010

Keywords:
Thin-film
Dye-sensitized solar cell
Layer-by-layer assembly

ABSTRACT

Polyacrylate sodium (PAAS)/titania (TiO_2) multilayers have been fabricated through the electrostatic layer-by-layer assembly technique. The composite films display an excellent photovoltaic performance after sintering and sensitization by cyanine dye (CD), which can be applied in dye-sensitized solar cells. The properties of PAAS/TiO_2 multilayers are investigated by ultraviolet–visible spectroscopy (UV–vis), X-ray photoelectron spectroscopy (XPS), X-ray diffraction analysis (XRD), Thermogravimetric analysis (TGA), and photovoltaic measurements. The results indicate that the thermal stability of the PAAS has a direct influence on the performance of dye-sensitized solar cells. The energy conversion efficiency of approximately 1.29% was obtained for dye-sensitized solar cell with TiO_2/PAAS (40 bilayers) as precursor film. In addition, the composite films also show a good self-cleaning property for photocatalytic degradation of methylene blue.

1. Introduction

Dye-sensitized solar cells (DSSCs) with high energy conversion efficiency and low cost have been widely investigated [1–3]. Study of DSSCs includes dye synthesis electrode material selection and anode preparation. Although DSSCs with high power conversion efficiencies (up to 11%) have been achieved [3], the development of new materials and suitable device architectures is needed for further improvement in various properties. As we know, the anode of DSSCs can be fabricated by several methods such as casting, doctor blading, screen printing, dip coating and chemical vapor deposition [4]. Recently, Chen et al. [5] reported that nanopowders synthesized by a flat-flame chemical vapor condensation method were used as the anodes of dye-sensitized solar cells (DSSCs), and a potentially >8% efficiency is projected for the DSSCs when the anodes are made solely of the synthesized nanopowders. Lokhande et al. [6] reported that various metal oxide thin-films have been obtained by chemical deposition methods. These simple and inexpensive chemical bath deposition, successive ionic layer adsorption and reaction, spray pyrolysis and electrodeposition methods are suitable for application in photoelectrochemical cells, LPG sensors, supercapacitors and dye-sensitized solar cells.

The electrostatic layer-by-layer assembly (ELBL) technique is one of the most important fabrication methods of thin-film [7]. The ELBL assembly technique has been widely used to fabricate compounds such as nanoparticles (NPs) [8], clays [9], and organic matter [10]. Recently, we have fabricated Chitosan/tungstosilicate acid-silver and phosphotungstic acid/silver thin-films by ELBL [11]. Compared with other techniques for the construction of NPs-polymer composite film, this method only needs simple equipment and can fabricate highly homogeneous composite films. Several research groups have employed the ELBL method to assemble TiO_2 nanoparticles/polyelectrolytes films for potential applications in optical, electronic, and mechanical devices [12]. Besides usages mentioned above, the ELBL deposition technique has also been reported for the preparation of dye-sensitized solar cell with poly(dimethyldiallylammonium chloride) PDAC/TiO_2 (200 bilayers) as precursor film and an efficiency of 7.2% was obtained under 1 sun at simulated AM 1.5 direct irradiation [13]. However, it is seldom reported that the TiO_2 films prepared by the ELBL technique together with other dyes except ruthenium complexes can be sensitized in DSSCs.

In this study, titania (TiO_2)/polyacrylate sodium (PAAS) composite films were assembled through the ELBL method and applied in dye-sensitized solar cells. The deposition process during the fabrication of the homogeneous film was monitored by UV–vis spectrometry. The composition of the $\{PAAS/TiO_2\}_n$ multilayer films was characterized by X-ray photoelectron spectrometer. The effect of PAAS on the overall device efficiency of the solar cell is discussed. And the mechanism of photocatalytic degradating methylene blue by the TiO_2 nanoparticle multilayers is investigated as well.

* Corresponding author. Tel.: +86 551 5108090; fax: +86 551 5108702.
E-mail addresses: s_yuhua@163.com, zhlisuzh@163.com (Y.H. Shen).

0925-8388/$ – see front matter © 2010 Elsevier B.V. All rights reserved.
doi:10.1016/j.jallcom.2010.06.077

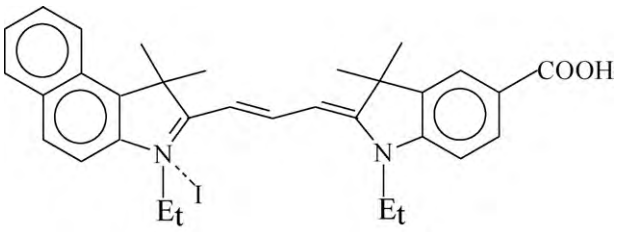

Fig. 1. The molecular structure of CD.

2. Experimental

2.1. Materials

Sodium polyacrylate (PAAS, $M_w \geq 3000$) ($Ti(OC_4H_9)_4$) nitric acid (HNO_3), ammonia ($NH_3 \cdot H_2O$) were all A.R. grade and obtained from Shanghai Reagent Co. Propylene carbonated (PC) was dried by molecule sieve and then distilled before use. ITO conducting glass (Indium doped SnO_2, sheet resistance 20 $\Omega\,cm^{-2}$, transmission of more than 75% in the visible spectrum region) was purchased from Benbu Huayi Conductive Film Glass Co., Ltd. in Anhui province. A Milli-Q water with an average resistivity of 18 $M\Omega\,cm^{-1}$ and pH = 6.5 was used for all experiments. The assembly of multilayer films was carried out in a dust-free box at the temperature of $18 \pm 1\,^{\circ}C$. CD dye was synthesized and purified. The molecular structure was confirmed by ^1H NMR as shown in Fig. 1.

2.2. Synthesis of TiO_2 nanoparticles

A 300 mL HNO_3 (pH = 1) solution was added to a 500 mL flask. Then, 25 mL tetrabutyl titanate was added dropwise into the above solution under vigorous stirring. The solution was heated to and maintained at 80 °C for 8 h. At last, the transparent yellow TiO_2 sol was obtained and conserved at 4 °C. TiO_2 sol was sintered at 500 °C for 30 min, and then used as the sample for X-ray diffraction (XRD) measurement.

2.3. Layer-by-layer assembly of $\{PAAS/TiO_2\}_n$ multilayer film and DSSC electrode fabrication

TiO_2 nanoparticles are amphoteric in nature and the charge can be controlled by adjusting the pH value. TiO_2 is positively charged in pH = 1 aqueous solution, which can attract negatively charged PAAS in ELBL self-assembly techniques. The fabrication of the multilayer film was carried out in the following way: the hydrophilized substrate was first immersed into TiO_2 solution for 10 min, followed by washing with Millipore water. After that, the sample was washed with Millipore water and blown with nitrogen gas. The TiO_2 coated substrate was then immersed into 2 mg mL^{-1} PAAS solution for 10 min following with washing and blowing steps mentioned above. The adsorption and rinsing steps were repeated until the required number of bilayers was obtained. The polyelectrolyte/TiO_2 composite films were calcinated at 550 °C for 30 min to get sintered TiO_2 nanoporous films. In order to minimize rehydration of TiO_2 from moisture in the ambient air, the electrodes were soaked in 1 mmol L^{-1} CD ethanol solution for 12 h while cooling to about 80 °C from the annealing step.

2.4. Photocatalytic activities of TiO_2 nanoporous films

Methylene blue (MB) was used as model contaminant. Sintered TiO_2 nanoporous film with 20 bilayers was immersed in 0.01 mmol L^{-1} MB solution for 10 min. Contaminated samples were irradiated with ultraviolet light (Pyrex filter, >280 nm, 450 W Hanovia medium pressure lamp). The amount of MB remaining in the multilayer was monitored by measuring the UV–vis spectra and comparing the absorbance measured at 665 nm.

2.5. Preparation of DSSC and photovoltaic measurements

After dye sensitization, the electrodes were washed by ethanol and dried in air. The current–voltage curves were obtained at a scan rate of 5 mV s^{-1} in a two-electrode arrangement, which is identical with loading a variable resistor. A sandwiched photovoltaic device was prepared with the CD-sensitized TiO_2 electrode, a platinized ITO glass as counter electrode and 0.3 mol L^{-1} LiI/0.03 mol L^{-1} I_2 PC solution as electrolyte. The electrolyte was introduced into the interior of the solar cell via capillary forces. The active area of the solar cells is 0.6 cm^2, and the thickness of the TiO_2 nanocomposite film is approximately 175 nm from FESEM image. The current–voltage (I–V) measurement was measured under AM 1.5G at 58.5 mW cm^{-2} illumination. A 150 W xenon lamp combining high-intensity grating monochromator was served as the light source. In addition, a 10 cm water filter and a 350 nm cut-off filter were placed in the beam.

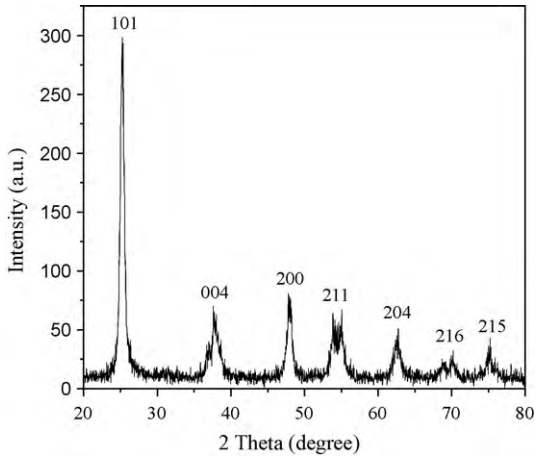

Fig. 2. XRD pattern of TiO_2 nanoparticles.

2.6. Characterization

XPS measurements of a multilayer film were carried out on an ESCALAB 250 X-ray photoelectron spectrometer (American Thermo Co.), at a pressure greater than 10^{-6} Pa. The general scan, C_{1s}, Ti_{2p} and O_{1s} core-level spectra were recorded with unmonochromatized Al K_α radiation (photon energy = 1486.6 eV). XRD analysis of the TiO_2 nanoparticles was performed on a MAP18AHF instrument (Japan MAC Science Co.). Thermogravimetric analysis (TGA-50H analyzer, Japan SHIMADZU) was carried out in ambient atmosphere, which mimics the sintering condition. TGA curves were recorded by heating solid samples (~5 mg) at a rising rate of 10 °C/min up to 800 °C.

3. Results and discussion

The surface charge on colloidal TiO_2 nanoparticles is crucial for the assembly of the polyelectrolyte/TiO_2 composite films by ELBL technique. In principle, since the isoelectric point (pI) of an aqueous colloidal TiO_2 dispersion varies from 4.5 to 6.8 [14,15], which strongly depends on the size of particles and counterions used. Bare TiO_2 nanoparticles may serve as an amphoteric material depending on the pH of the dispersing agent. When the pH of the medium is higher than the pI of TiO_2, the surface charge of TiO_2 particles is negative. Otherwise, it is positive. In this work, TiO_2 nanoparticles were synthesized under an acidic medium, which are positively charged and can adsorb negatively charged PAAS to form PAAS/TiO_2 multilayered films.

Fig. 2 shows the XRD pattern of TiO_2 nanoparticles. Seven diffraction peaks are identified in the diffraction pattern. The positions of the peaks (25.4°, 37.61°, 47.84°, 54.14°, 62.75°, 69.77°, 75.23°) are assigned to (1 0 1), (0 0 4), (2 0 0), (2 1 1), (2 0 4), (1 1 6), and (2 1 5) planes of TiO_2 crystals (JCPDS, 21-1272), respectively, which were reported previously in the literature for anatase TiO_2 [16]. The broadening of these peaks clearly indicates that the TiO_2 particles are possible nanocrystalline.

UV–vis spectroscopy was used to monitor the assembly process of PAAS/TiO_2 multilayer film on a quartz glass. Fig. 3 exhibits the UV–vis absorption spectra of multilayer films deposited on a quartz slide at 200–800 nm. The spectra show a peak at 244 nm and an absorption band in the range of 200–300 nm, respectively. There is no absorption for PASS in the range of 200–800 nm. The absorption at 244 nm can be assigned to the characteristic peaks of TiO_2. The above results clearly reveal that the TiO_2 nanoparticles were fabricated into the composite film. The inset of Fig. 3 shows a plot of the absorption intensity at 244 nm against the number of assembled bilayers. The absorption peak increases linearly with the number of assembled bilayers, which suggests the TiO_2 NPs in the composite film grow regularly and uniformly. Such a behavior could be observed in many layer-by-layer deposition systems due to electrostatic interaction [17–19].

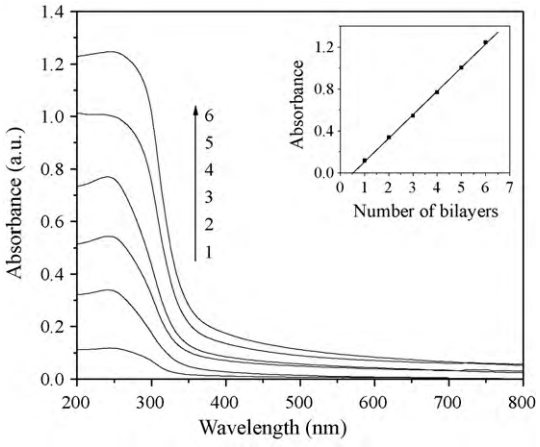

Fig. 3. UV–vis absorption spectra of $\{PAAS/TiO_2\}_n$ multilayer films on quartz substrates (the curves from bottom to top, corresponding to adsorption of 1, 2, 3, 4, 5, and 6 bilayers), The inset of Fig. 3 shows a plot of the absorbance intensity at 244 nm against the number of the bilayers.

XPS measurements were performed to identify elemental composition of multilayer films deposited on the single-crystal silicon substrate. The C_{1s} core-level spectrum recorded from the film is shown in Fig. 4a, and it can be stripped into four main chemically distinct components at 284.65, 288.71, 286.25, and 287.65 eV, respectively. The 284.65 and 288.71 eV peaks are attributed to the carbon bound and carboxylate carbon of PAAS, respectively. The 286.25 eV peak is ascribed to the carbon bound to the hydroxyl group from residual butanol [20]. The 287.65 eV BE peak can be assigned to the carbonyl carbon resulting from the hydroxyl and carboxylate bonding present in TiO_2. Fig. 4b shows the Ti_{2p} core-level spectrum. The Ti_{2p} peak resolves into two spin-orbit components. The peak occurs at the binding energy of 458.8 corresponding to Ti^{+4}. Fig. 4c shows the O_{1s} spectrum. The 530.02 eV BE peak is ascribed to the Ti–O bonding present in TiO_2. The 531.18 eV BE peak is assigned to the oxygen atom bound to the carboxylate group of PAAS, or hydroxyl group from resulting butanol or H_2O. The results of XPS and UV–vis spectra confirm that the TiO_2 and PAAS exist in the composite film.

Fig. 5a shows the morphology of TiO_2 multilayered film after sintering. It is clearly observed that the TiO_2 film is composed of a three-dimensional network of interconnected nanoparticles with an average size of 15 nm. Comparing with the size of TiO_2 colloid, the annealing at 450 °C did not significantly change the size of particles. A similar observation was reported by Kumar's [13] and Grätzel's group [1]. Fig. 5b clearly shows that the thickness of TiO_2 nanocomposite film is about 175 nm.

The self-cleaning properties of TiO_2 nanoparticle-based multilayers have been tested under UV irradiation [12a]. Glass substrate coated with TiO_2 nanoparticle-based multilayers was contaminated using methylene blue (MB). After UV irradiation, the amount of MB remaining in the films as a function of time is shown in Fig. 6. Nearly 85% of the MB in the TiO_2 nanoparticle-based multilayers decomposed after 6 h of UV irradiation. It indicates that the TiO_2 thin-film has photocatalytic degradation and self-cleaning properties.

Another key component of the nanocomposite films is the polyelectrolytes, which are insulator. When the materials are not completely burn away in the high-temperature sintering process, the residuals left inside the TiO_2 film can increase the internal resistance of the solar cell and resulting reduce the photocurrent output. According to this consideration, the thermal stability of the polyelectrolyte was tested by TGA (as shown in Fig. 7). It can be seen that the weight loss of PAAS is ca. 47% under the sintering temperature of 550 °C. Kumar et al. also observed the similar phenomenon that there were more residuals of the polyanions left in the final TiO_2 electrodes after sintering at 550 °C [13]. Due to the insulating property of the residuals inside the final TiO_2 electrode, the more

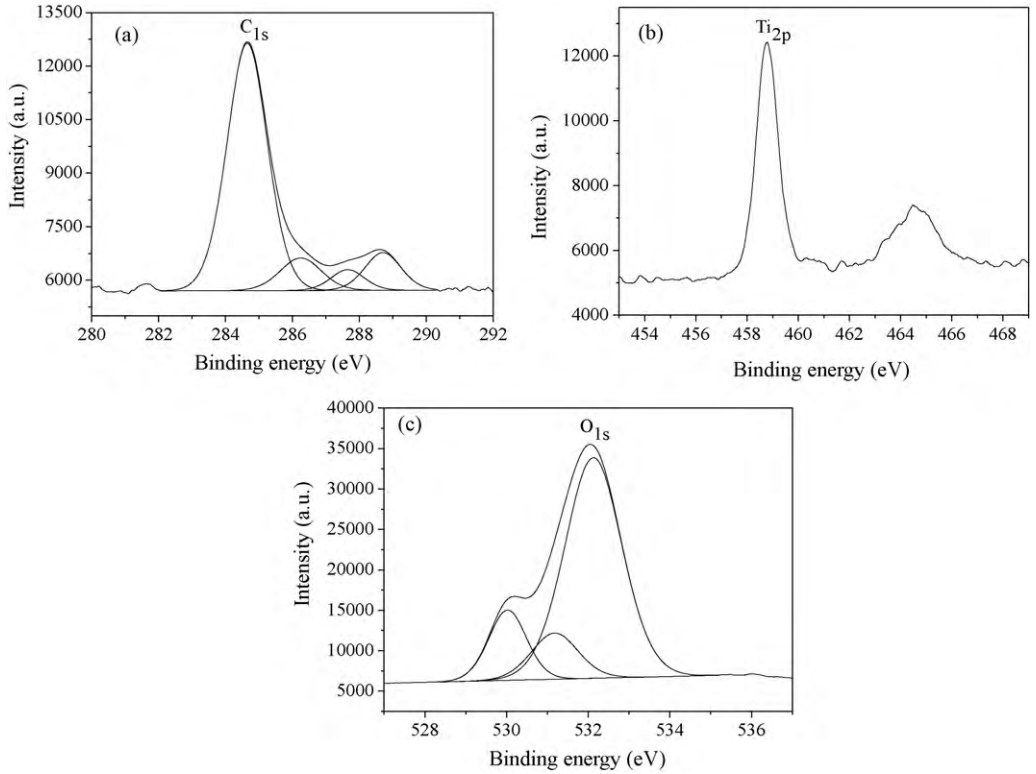

Fig. 4. XPS core-level spectra recorded from $\{PAAS/TiO_2\}_{10}$ multilayer films deposited on Si substrate (a) C_{1s}, (b) Ti_{2p}, (c) O_{1s}.

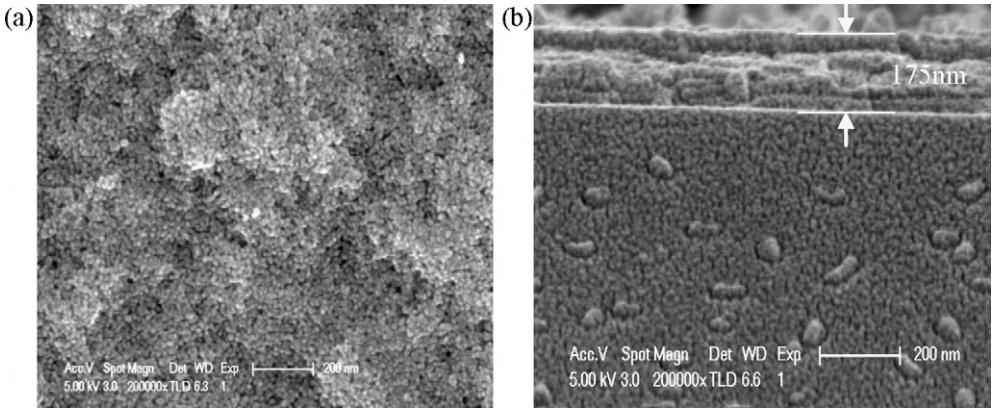

Fig. 5. FESEM images of the surface (a) and cross-section (b) of TiO_2 nanocomposite film after sintering.

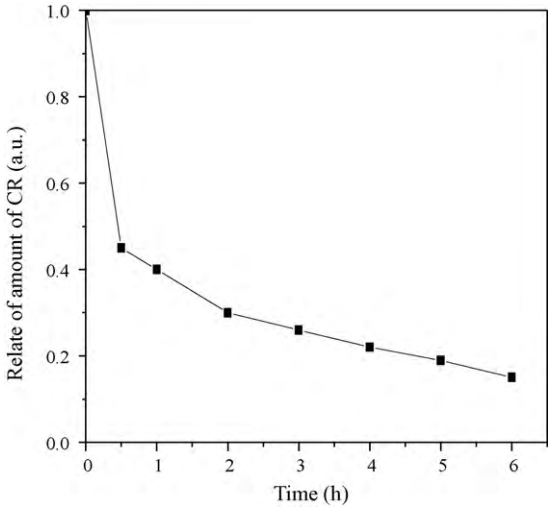

Fig. 6. The relative amount of methylene blue remaining in a 20 bilayer TiO_2 multilayer as a function of time under UV irradiation.

the residual film has, the poorer the performance of the cell gets. When high-performance dye-sensitized solar cells were prepared, the TiO_2 paste with addition of carbon wax with 40% of TiO_2 weight was spread on the conducting glass. Carbon wax M-20,000 was removed from the film by sintering at 450 °C and electronic contact among nanoparticles was formed. Therefore, it can be concluded that the thermal stability of the polyelectrolyte plays a major role

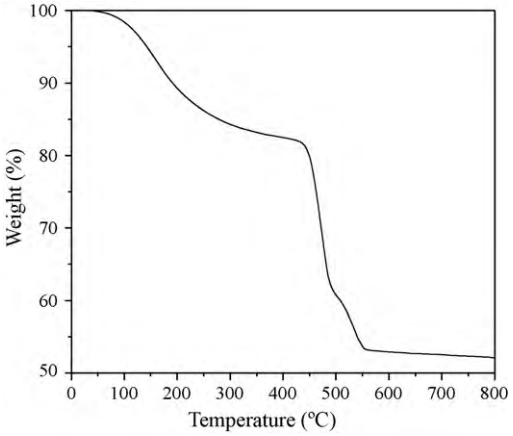

Fig. 7. TGA of PAAS under an air atmosphere, the heating rate is 10 °C/min.

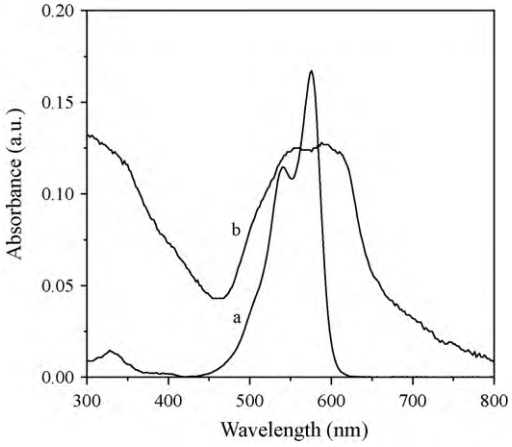

Fig. 8. (a) UV–vis absorption spectrum of CD in absolute ethanol solution, absolute ethanol solution as reference; (b) absorption spectrum of dye-sensitized TiO_2 nanostructured film deposited on conducting glass, SnO_2 conducting glass as reference.

in the performance of the cell with polyion/TiO_2 nanocomposite films.

Fig. 8 shows UV–vis absorption spectra of CD in absolute ethanol solution (a) and the dye-sensitized TiO_2 nanostructured film (b). There are two absorption peaks at 540 and 576 nm in visible region (as shown in Fig. 8a). The main absorption ranges from 490 to 600 nm. From Fig. 8b, it can be observed that the absorption range of

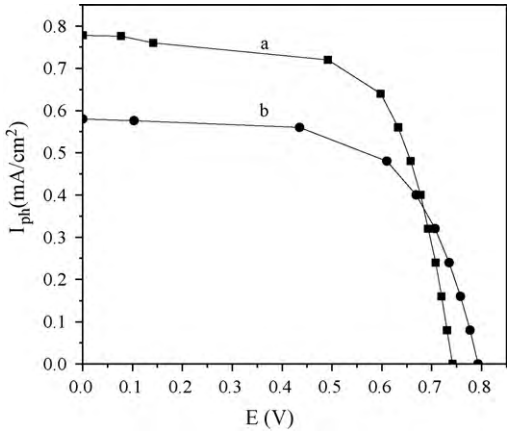

Fig. 9. Photocurrent density–voltage curves of solar cell made from bare TiO_2 film synthesized by coated method (a) and composites synthesized by LbL method (b) under 58.5 mW cm^{-2} illumination.

dye-sensitized TiO_2 nanostructured film is wider than CD in absolute ethanol solution, which results from the interlocking bridge between CD and TiO_2 as ester-like bond.

Fig. 9 shows photocurrent density–voltage curves of solar cells with bare TiO_2 film synthesized by coating method (a) and composites synthesized by LbL method (b) under 58.5 mW cm^{-2} illumination. The energy conversion efficiencies of the cells with ITO/TiO_2/CD structure and ITO/TiO_2/CD LbL structure are 1.25 and 1.29%, respectively. Comparing with the film with bare TiO_2, there is no distinct increase in LbL film cell. The conversion efficiency of the DSC obtained by the above two methods is lower than the 5% (for cyanine dyes) reported for other published materials [21]. We think that the lower thickness of the TiO_2 film might be the major reason [13].

4. Conclusions

In this study, the ELBL technique has been used as an alternative approach to fabricate nanocrystalline TiO_2 electrodes for DSSCs applications. An efficiency of 1.29% was obtained for the solar cell with TiO_2/PAAS as precursor film. Thermogravimetric analysis of PAAS shows that the thermal stability of the polyelectrolytes may have a direct effect on the overall device efficiency. Moreover, TiO_2 multilayers can be used for photocatalytic degradation of methylene blue, and they exhibit self-cleaning function. The advantages of the ELBL technique such as versatility, thickness, composition, and porosity control are expected to provide many new opportunities for the design and fabrication of efficient dye-sensitized solar cells.

Acknowledgements

This work was supported by the National Natural Science Foundation of China (20871089, 20871001 and 20731001), the Important and Key Projects of Anhui Provincial Education Department (ZD2007004-1, KJ2010ZD09 and KJ2007A076), and the Research Fund for the Doctoral Program of Higher Education of China (20070357002), and the Foundation of Key Laboratory of Environment-friendly Polymer Materials of Anhui Province.

References

[1] M. O'Regan, Grätzel, Nature 353 (1991) 737–740.
[2] E. Indrea, S. Dreve, T.D. Silipas, G. Mihailescu, V. Danciu, V. Cosoveanu, A. Nicoara, L.E. Muresan, E.J. Popovici, V. Popescu, H.I. Nascu, R. Tetean, J. Alloys Compd. 483 (2009) 445–449.
[3] M.K. Nazeeruddin, F.D. Angelis, S. Fantacci, A. Selloni, G. Viscardi, P. Liska, S. Ito, B. Takeru, M. Grätzel, J. Am. Chem. Soc. 127 (2005) 16835–16837.
[4] (a) H.J. Snaith, C.S. Karthikeyan, A. Petrozza, J. Teuscher, J.E. Moser, M.K. Nazeeruddin, M. Thelakkat, M. Grätzel, J. Phys. Chem. C 112 (2008) 7562–7566; (b) H. Chang, H.M. Wu, T.L. Chen, K.D. Huang, C.S. Jwo, Y.J. Lo, J. Alloys Compd. 495 (2010) 606–610.
[5] Y.J. Chen, M.C. Hsu, Y.C. Cai, J. Alloys Compd. 490 (2010) 493–498.
[6] C.D. Lokhande, A.M. More, J.L. Gunjakar, J. Alloys Compd. 486 (2009) 570–580.
[7] G. Decher, Science 277 (1997) 1232–1237.
[8] S. Bhattacharjee, M.L. Bruening, Langmuir 24 (2008) 2916–2920.
[9] A. Mamedov, J. Ostrander, F. Aliev, N.A. Kotov, Langmuir 16 (2000) 3941–3949.
[10] L. Shen, N. Hu, Biomacromolecules 6 (2005) 1475–1483.
[11] L. Zhang, Y.H. Shen, A.J. Xie, S.K. Li, C. Wang, J. Mater. Chem. 18 (2008) 1196–1203.
[12] (a) D. Lee, M.F. Rubner, R.E. Cohen, Nano Lett. 6 (2006) 2305–2312; (b) N. Sakai, G.K. Prasad, Y. Ebina, K. Takada, T. Sasaki, Chem. Mater. 18 (2006) 3596–3598.
[13] J.-A. He, R. Mosurkal, L.A. Samuelson, L. Li, J. Kumar, Langmuir 19 (2003) 2169–2174.
[14] C. Kormann, D.W. Bahnemann, M.R. Hoffmann, J. Phys. Chem. 92 (1988) 5196–5201.
[15] J. Zhao, H. Hidaka, A. Takamura, E. Pelizzetti, N. Serpone, Langmuir 9 (1993) 1646–1650.
[16] C.J. Barbé, F. Arendse, P. Comte, M. Jirousek, F. Lenzmann, V. Shklover, M. Grätzel, J. Am. Ceram. Soc. 80 (1997) 3157–3171.
[17] N. Sakai, G.K. Prasad, Y. Ebina, T. Sasaki, Chem. Mater. 18 (2006) 3596–3598.
[18] L. Zhang, Y.H. Shen, A.J. Xie, S.K. Li, Y.M. Li, J. Mater. Chem. 19 (2009) 1884–1893.
[19] C. Lu, I. Donch, M. Nolte, A. Fery, Chem. Mater. 18 (2006) 6204–6210.
[20] J.F. Moulder, W.F. Stickle, P.E. Sobol, K.D. Bomben, in: J. Chastain (Ed.), Handbook of X-ray Photoelectron Spectroscopy, 2nd ed., Perkin-Elmer Corporation Physical Electronics Division, Eden Prairie, Minnesota, 1992.
[21] Z.S. Wang, F.Y. Li, C.H. Huang, J. Phys. Chem. B 105 (2001) 9210–9217.